Australian Journal of Basic and Applied Sciences, 10(18) December 2016, Pages: 290-302

AUSTRALIAN JOURNAL OF BASIC AND APPLIED SCIENCES

ISSN:1991-8178 EISSN: 2309-8414
Journal home page: www.ajbasweb.com

Novel Approaches for Inferring Electron Density & Electron Temperature from Langmuir Probe's I-V Curves Measured in the Afterglow of Pulse-Modulated ICP Argon Plasma.

[1,2]Mansour ElSabbagh

[1]*Plasma & Laser Lab. Department of Physics, Faculty of Sciences (male), Al-Azhar University. Nasr City, Cairo, Egypt.*
[2]*Al-Azhar University Center of Plasma Technology (AUCPT), Faculty of Sciences (male), Al-Azhar University. Nasr City, Cairo, Egypt.*

Address For Correspondence:
Mansour ElSabbagh, Al-Azhar University, Department of Physics, Faculty of Sciences (male), Nasr city, Cairo, Egypt.
E-mail:mansouram2004@yahoo.com

ARTICLE INFO

Article history:
Received 19 September 2016
Accepted 10 December 2016
Published 31 December 2016

Keywords:
Electron density, electron temperature, Langmuir probe, pulse-modulated ICP discharge, afterglow, argon plasma.

ABSTRACT

Langmuir probes are commonly used to diagnose different types of plasmas because they are experimentally simple and because many important plasma parameters can be estimated from them. In literature, different probe theories are used to analyze its I-V characteristics to deduce the plasma parameters from them. In this article and for the first time as far as we know, two novel approaches have been proposed and checked to infer n_e & T_e from the electron repelling current and electron saturation current regions of the measured Langmuir probe's I-V curve respectively. The time resolved electron density (n_e) & electron temperature (T_e) of pulse-modulated inductively coupled plasmas in argon have been measured in the afterglow using compensated-Langmuir probe. The measurements were performed for averaged RF powers of 300 & 500 W at frequency of 13.56 MHz, duty cycle of 50 %, and pulse repetition frequency of 12.5 kHz. Argon gas pressure was 20 mTorr and flow rate of 132 sccm. The electron density in the afterglow showed a peak in its value at elapsed time of 5 μs, which might be attributed to Penning ionization, after that it was monotonically decreased. The electron temperature was rapidly decreased in the first 10 μs and after that it was monotonically decreased. Inferring n_e from the electron repelling current region has been proved to be a reliable approach, and it is the only approach to deduce the electron densities of cold & hot groups of plasmas having bi-Maxwellian electron energy distribution function. Inferring T_e from the electron saturation current region has been found to be reliable method only in case of plasmas having Maxwellian electron energy distribution function.

INTRODUCTION

Inductively coupled plasma (ICP) sources can produce a high density (10^{10} to 10^{12} cm^{-3}) and uniform plasma in low-pressure gases without the need of external magnetic fields (Economou, 2004, Liu *et al*., 2015, Ramamurthi *et al*., 2003). Commercial reactors operate at 1-50 mTorr pressure range and 0.2-2.0 kW power levels. Possible applications include deposition and etching of a wide variety of materials such as SiO_2, metals, and low-*k* dielectrics. Pulsed-modulated ICP sources have already shown a capability for improving etching and deposition processes that are being developed for the manufactures of semiconductor devices in the future (Despiau-Pujo *et al*., 2013). By rapidly switching the discharge power on and off, damage induced by plasma process can be suppressed or eliminated (Malyshev and Donnelly, 2000), and the composition of radicals in the gas phase can be better controlled, leading to improved central selectivity in etching (Sugai *et al*., 1995, Petit-

To Cite This Article: Mansour ElSabbagh., Novel Approaches for Inferring Electron Density & Electron Temperature from Langmuir Probe's I-V Curves Measured in the Afterglow of Pulse-Modulated ICP Argon Plasma.. ***Aust. J. Basic & Appl. Sci.,*** *10(18): 290-3020, 2016*

Australian Journal of Basic and Applied Sciences, 10(18) December 2016, Pages: 290-302

Etienne *et al*., 2010) and film composition in deposition (Watanabe *et al*., 1988). A complete understanding of how the main plasma parameters change in the afterglow is?, therefore, of primary importance for plasma processing design and optimization.

Langmuir probes (Hershkowitz, 2016) are frequently used in plasma discharges because they are experimentally simple and because many important plasma parameters can be estimated from them: ion and electron densities, electron temperature, electron energy distribution function, and plasma potential. Several excellent publications concerning Langmuir probes have appeared during the last 50 years (Laurent *et al*., 2013, Chen, 1965, Swift and Schwar, 1971, Hershkowitz, 1989, Meshcheryakova *et al*., 2015). The interpretation of probe data in RF discharges is complicated by plasma potential fluctuations. Many techniques have been developed to minimize RF interference (Meshcheryakova *et al*., 2015, Hershkowitz *et al*., 1988, Gagne and Cantin, 1975, Paranjpe *et al*., 1990, Sudit and Chen, 1994, Singh, 2004). Among those techniques is the passive compensation technique (Sudit and Chen, 1994, Singh, 2004)) which was adopted in the current work to measure the correct probe current-voltage characteristics. The plasma parameters are inferred from the probe current-voltage characteristics regions by different approaches (Hershkowitz, 2016, Lee *et al*., 2016, Chen, 1965, Swift and Schwar, 1971, Hershkowitz, 1989).

In this article, a home-made compensated Langmuir probe was constructed and used to measure the temporal evolution of the plasma parameters in the afterglow of pulse-modulated argon ICP discharge. Two novel approaches to infer the electron density and electron temperature from the electron repelling current & electron saturation current regions respectively were proposed and were used for the first time as far as we know. A comparison of the plasma parameters deduced from the compensated probe current-voltage characteristics using different approaches was presented in the current work.

This article is organized as follows. After this introduction, the probe theory and the different approaches of deducing the plasma parameters are reviewed in the method section strengthen on the possibility of using two novel approaches to deduce the electron temperature and the electron density. Two sections are devoted for the experimental setup and the experimental results and their discussion. Final section of the article is committed to a conclusion of the article's work.

Method:

Electrostatic probes are undisputedly the oldest and most widely used diagnostic tools in plasma physics. The technical and first theoretical explanation of the electrostatic probe was developed by I. Langmuir and hence it is widely known as Langmuir probe. Principally in its simplest form a Langmuir probe is just a conducting wire inserted in the plasma, whose current-voltage characteristic I-V (when the wire is biased) is measured with respect to reference electrode. The resulting probe characteristic is analyzed using an appropriate probe theory which creates a connection between the measured I-V characteristic curve and the parameters of the undisturbed plasma. The plasma parameters which can easily be obtained using measured characteristic curve and appropriate probe theory are floating potential (V_f), plasma potential (V_p), electron temperature (T_e), electron density (n_e) and electron energy distribution function ($f(\varepsilon)$).

Probes are easy to construct and are very flexible with the dimension but the simplicity in the technical part has to compromise a lot with extremely complicated theories involved. Another and the biggest problem associated with probe measurements is due to its physical presence in the discharge. The plasma has a basic nature to shielding any external perturbation (within some Debye length) but in reality this shielding effect is never so localized (Chen, 1983). So to say physical presence of probe eventually affects a lot to the surrounding discharge condition. If the electron density is high, the influence on the measurements is negligible (Peter Messerer, 2010). On the other hand advantages over diagnostic tools like Thomson scattering, microwave interferometer and optical emission spectroscopy are, its low cost and its ability to do local measurements. However, the other techniques either are very high budget or provide only the volume averaged parameters.

a- Langmuir probe theory:

Once the probe tip is inserted into the plasma it will be surrounded by a plasma sheath leaving the bulk plasma (after the sheath edge) at a positive plasma potential (V_p). The applied DC potential to the tip with respect to the sheath edge potential (i.e. plasma potential) can be represented by $U=V_a-V_p$, where V_a is the applied DC potential. Furthermore, at a floating state the voltage drop across the sheath acts as a barrier to approaching electrons (or rather attract ions), making ion and electron flux equal at the floating potential (V_f). In the I-*V* curve (fig. 1) the point of equal ion-electron flux can be identified at the point where magnitude of current is zero. For the complete explanation and understanding of the *I-V* curve, it is divided into three regions according to the applied voltage (V_a).

a-i) Ion saturation current ($I_{i,s}$) current ($V_a < V_f$ and $U << kT_e/e$):

The voltage applied to the probe tip in this region is negative with respect to the floating potential (see area A of fig. 1). Also the value of *U* (potential barrier for the electrons) is much larger than the electron temperature,

so that not even the fastest electrons can reach the probe tip. Hence, electron contribution to the current in this region is zero. On the other hand in this region because of high negative potential across the sheath the positive ions are attracted to the probe surface and contribute to the current flow. The probe acts like an attracting electrode for the ions, and making the tip even further negative will soon saturate the ion current. For low temperature plasmas where T_i (ion temperature) $\ll T_e$ the ion saturation current is approximated close to the floating potential by the Bohm relation (Chen, 1983, Lobbia and Gallimore, 2010)

$$I_{i,s} = I_{Bohm} = 0.6 n_i e A_p \sqrt{\frac{kT_e}{m_i}} \qquad (1)$$

Where e, A_p, k, n_i & m_i are electron charge, probe surface area, Boltzmann constant, ion density and ion mass respectively.

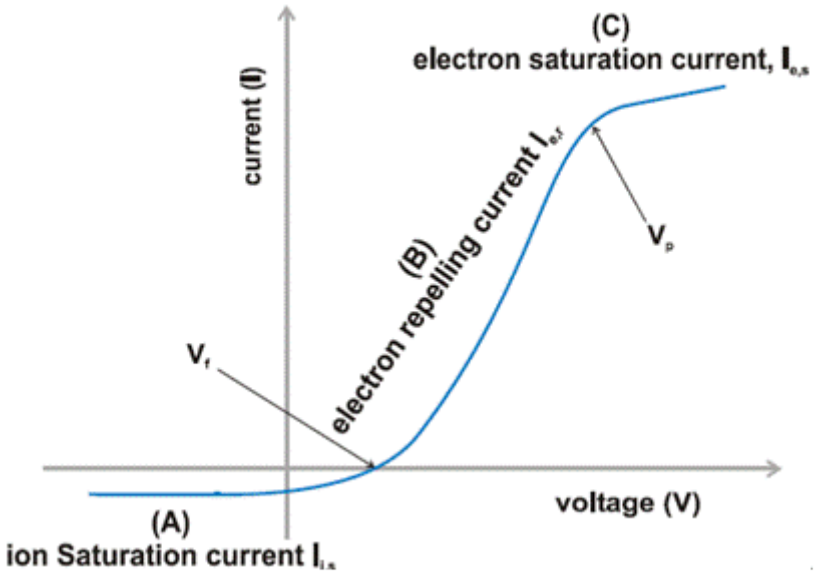

Fig. 1: Langmuir probe's I-V characteristics curve.

a-ii) Electron repelling current ($I_{e,r}$) region ($V_f < V_a \leq V_p$ and $U < kT_e/e$) :

Sometimes this region is called electron retardation region (see region B offig.1). When $V_a \approx V_p$ a kink is observed in the probe I-V characteristics, this is also referred as the knee. This is occurs because of the collapse and reversal of the sheath from an electronegative ($V_a > V_p$) to an electropositive sheath ($V_a < V_p$). At $V_a = V_p$ the currents arriving at the probe of surface area A_p are simply the random thermal currents ($I_{e,s}$) given by $I_{e,s} = (1/4) e A_p n_e v_{th}$, where v_{th} is the electron thermal speed given by $v_{th} = (8kT_e / \pi m_e)^{1/2}$. In low-temperature non-equilibrium plasmas $T_e >> T_i$ and $m_i >> m_e$ so that I_e (electron current) >> I_i (ion current). If the plasma electrons have a population of low energy electrons then for $V_a < V_p$ electrons are rapidly repelled such that a maximum in the gradient of the I-V characteristics appear close to V_p. This corresponds to the maximum in the dI_p/dV_a and zero-crossing in the d^2I_p / dV_a^2. Therefore, the first zero-crossing of d^2I_p / dV_a^2 is used to measure the plasma potential.

For a Maxwellian plasma the repulsion of electrons allows their temperature to be inferred provided the ion current is negligible or can be subtracted. A common method of subtracting the ion current is by linear extrapolation from the ion saturation current region ($V_a < V_f$). The electron current to the probe may be written as

$$I_{e,r} = I_{e,s} \exp\left(\frac{e(V_a - V_p)}{kT_e}\right) = \frac{1}{4} n_e e A_p \left(\frac{8kT_e}{\pi m_e}\right)^{1/2} \exp\left(\frac{e(V_a - V_p)}{kT_e}\right)$$

$$I_{e,r} = \frac{e^{3/2} A_p}{(2\pi m_e)^{1/2}} n_e T_e^{1/2} \exp\left(\frac{V_a - V_p}{T_e}\right), \text{where } T_e \text{ in volts}$$ By talking the natural log of both sides of the equation one can get

$$\mathrm{LnI_{e,r}} = \left[\mathrm{Ln}\left(\frac{\mathrm{e^{3/2} A_p}}{\mathrm{(2\pi m_e)^{1/2}}} \mathrm{n_e T_e^{1/2}} \right) - \frac{\mathrm{V_p}}{\mathrm{T_e}} \right] + \frac{1}{\mathrm{T_e}} \mathrm{V_a} \qquad (2)$$

According to equation 2 if $\mathrm{Ln_{e,r}}$ is plotted against V_a a straight line is obtained and its gradient is equal to the reciprocal if T_e (slope = $1/T_e$ where T_e in V). The intersection of the straight line (C_1) is equal to the terms between the two brackets of equation 2. From this intersection n_e can be deduced provided that V_p is known. From equation 2 the following relation can be easily obtained

$n_e = \frac{(2\pi m_e)^{1/2}}{e^{3/2} A_p} \times (slope)^{1/2} \times \exp\left(C_1 + (V_p \times slope)\right)$, which can be reduced to

$$n_e = 9.51 \times 10^{18} (slope)^{1/2} \times \exp\left(C_1 + V_p \times slope\right) \qquad (3)$$

To our knowledge, equation 3 has never been used before to deduce electron density in any kind of plasmas using Langmuir probes. If the plasma has bi-Maxwellian electron energy distribution function, then the electron density of each group of electrons can be deduced by using equation 3 because the plot of $\mathrm{Ln_{e,r}}$ against V_a will show two straight lines having two different slopes with two different intersections. Furthermore, the density of each group of electrons can be deduced using the intersections of the two straight lines.

a-iii) Electron saturation current ($I_{e,s}$) region ($V_a > V_p$ and $U > 0$):

This region sometimes called orbital motion limited (OML) region, region C in fig.1. In this region, V_a is even higher than the surrounding (plasma) potential V_p resulting in a negative sheath around the probe tip. Under this condition all the electrons reaching negative electron sheath get attracted and the current eventually saturates. For cylindrical probe and for thick plasma approximation ($r_s/r_p >> 1$, r_s is the probe sheath radius & r_p is the probe radius), the electron current I_e (at $U > 0$) is given by (Swift and Schwar, 1971)

$$\mathrm{I_e} = \mathrm{I_{e,s}} \frac{2}{\sqrt{\pi}} \left(1 + \frac{\mathrm{e(V_a - V_p)}}{\mathrm{kT_e}} \right)^{1/2} = \frac{\mathrm{A_p n_e e}}{\pi} \left(\frac{\mathrm{2kT_e}}{\mathrm{m_e}} \right)^{1/2} \left(1 + \frac{\mathrm{e(V_a - V_p)}}{\mathrm{kT_e}} \right)^{1/2} \qquad (4)$$

Equation 4 is valid only for $U > 2kT_e/e$, by squaring the two sides of equation 4 and rearranging its terms one can get

$$\mathrm{I_e^2} = \frac{\mathrm{2e^3 A_p^2 n_e^2}}{\pi^2 \mathrm{m_e}} \mathrm{V_a} + \frac{\mathrm{2e^3 A_p^2 n_e^2}}{\pi^2 \mathrm{m_e}} \mathrm{(T_e - V_p)}, \text{ where } \mathrm{T_e} \text{ in volts} \qquad (5)$$

If the square of the electron current is drawn against the probe biasing voltage V_a a straight line is obtained as can be seen from equation 5. From the slope of this straight line one can deduce n_e from equation 6.

$$\mathrm{Slope} = \frac{\mathrm{2e^3 A_p^2 n_e^2}}{\pi^2 \mathrm{m_e}} \rightarrow \mathrm{n_e} = (\mathrm{slope})^{1/2} \frac{\pi \mathrm{m_e}}{\sqrt{2} \mathrm{e^{3/2} A_p}}$$

$$\mathrm{n_e} = 8.43 \times 10^{18} \times (\mathrm{slope})^{1/2} \quad (\mathrm{m^{-3}}) \qquad (6)$$

The intersection of the straight line (C_2) that represents equation 5 is given by

$$C_2 = \frac{\mathrm{2e^3 A_p^2 n_e^2}}{\pi^2 m_e} \mathrm{(T_e - V_p)}, \text{ where } \mathrm{T_e} \text{ in volts} \qquad (7)$$

The electron temperature T_e can be deduced from equations 6 & 7 provided that the plasma potential V_p is known. T_e is given by

$$T_e = \frac{C_2}{slope} + V_p, \qquad \text{where } \mathrm{T_e} \text{ in volts} \qquad (8)$$

Also, to our knowledge it is the first time that T_e is deduced from equation 8.

b- Evaluation of plasma parameters:

b-i) Floating (V_f) and plasma (V_p) potentials:

The floating potential V_f is the potential at which an unbiased metallic surface would float in the plasma as a result of the developed sheath around it. In I-V characteristics curve of Langmuir probe, V_f corresponds to the probe bias voltage V_a for which the modulus of the electron repelling current ($I_{e,r}$) equals the ion saturation current ($I_{i,s}$) and hence is the point in a I-V curve where the current crosses zero.

V_p corresponds to the bias voltage where the plasma and probe are at the same potential (where $U = V_a - V_p = 0$). V_p defines the potential where the electron current changes from the electron repelling current ($I_{e,r}$) to the electron saturation current ($I_{e,s}$). In the "electron saturation region" electrons experience an attracting

Australian Journal of Basic and Applied Sciences, 10(18) December 2016, Pages: 290-302

potential whereas the probe delivers a repelling potential to the electrons in the "electron repelling region". The potential at point of change is defined as plasma potential and can easily be obtained by looking at the rate of change of the current with respect to the applied voltage. The maximum of the first derivative dI_p/dV_a or the zero crossing of the second derivative d^2I_p/dV_a^2 of the probe current with respect to the voltage is the way to find the plasma potential.

The exact determination of the plasma potential is very important since it sets the origin of the electron energy distribution function ($f(\varepsilon)$) in addition to deduce n_e & T_e from equations 3 & 8 , respectively, with higher accuracy. In the case of RF plasmas the second derivative method is preferred.

d^2I_p/dV_a^2 is obtained by numerically differentiating the measured I-V data according to the following steps. Firstly, the measured I-V data is smoothed using Savitzky-Golay algorithm built in commercially available OriginPro8 software. Secondly, the smoothed data is differentiated numerically using OriginPro8 software to get the first derivative. Finally, the first derivative data is smoothed using Savitzky-Golay algorithm before it is differentiated numerically once more to get the second derivative of the I-V data. The plasma potential (V_p) is deduced from the first zero crossing point of the second derivative of the electron current of the probe with the applied voltage.

b-ii) Electron energy distribution function f(ε):

The most salient feature of the probe I-V characteristics is the electron retarding region (where, $V_f < V_a < V_p$) which acts like an energy analyzer and carries information about $f(\varepsilon)$. In the case of r_s , $r_p << \lambda_e$ (mean free path of electrons) the collisions in the sheath will be rare, leaving the total energy of the electrons unchanged. Furthermore, the $f(\varepsilon)$ will also remain unchanged in the vicinity of the probe even due to the perturbation caused by the field. It has been firstly suggested by Langmuir (Langmuir, 1924) that the measurement of the second derivative as a function of applied voltage will enable to obtain $f(\varepsilon)$. Later Druyvesteyn proved this relation for the case of cylindrical and planar probes and proposed that this expression will also be applicable to any non-concave probe (Langmuir, 1924). $f(\varepsilon)$can be obtained using the following relation (Langmuir, 1924)

$$f(\varepsilon) = -\frac{2}{e^2 A_p}\left(\frac{-2m_e U}{e}\right)^{1/2}\frac{d^2 I_e}{dU^2} \qquad (9)$$

where $\varepsilon = eU$ & $\frac{d^2I_e}{dU^2} = \frac{d^2I_e}{dV_a^2}$.

Once $f(\varepsilon)$ is known the plasma parameters like electron density (n_e) and electron effective temperature (T_{eff}) can easily be obtained by using simple statistical formulas. The electron density can be obtained by integrating $f(\varepsilon)$ over all possible energies

$$n_e = \int_0^{\varepsilon_{max}} f(\varepsilon)d\varepsilon \qquad (10)$$

T_{eff} can be obtained from the following relation

$$T_{eff} = \frac{2}{3}\frac{\int_0^{\varepsilon_{max}} \varepsilon f(\varepsilon)d\varepsilon}{\int_0^{\varepsilon_{max}} f(\varepsilon)d\varepsilon} \qquad (11)$$

The units of n_e and T_{eff} deduced from equations 10 & 11 are m^{-3} and eV respectively, if ε units in these equations is eV.

b-iii) Electron temperature (T_e):

The electron temperature T_e for any plasma is only defined if the electron energy distribution function is Maxwellian whereas in non-Maxwellian plasmas (except bi-Maxwelian plasmas) the temperature term is meaningless and it is replaced by the effective temperature of the electrons (T_{eff}). T_e or T_{eff} can be inferred from the measured I-V characteristics curve from two regions

1- Electron repelling current region:

In this region, for non-Maxwellian electron energy distribution function, T_{eff} can be inferred from equation 11 provided that $f(\varepsilon)$ is deduced or measured. For Maxwllian electron energy distribution function T_e can be deduced using two methods. First method using measured or deduced $f(\varepsilon)$, T_e can be deduced using equation 11

where $T_e = 3/2\ T_{eff}$. Second method if the natural logarithm of the electron current (LnI_e) is drawn against the applied voltage of the probe tip (V_a) a straight line is obtained (according to equation 2) and its slope is equal to the reciprocal of T_e in eV units.

2- Electron saturation current region (OML region):

In this region, if the square of the probe current (I_p^2) is drawn against the applied voltage of the probe tip (V_a) a straight line is obtained and T_e could be deduced using equation 8 provided that the plasma potential is known. This is a novel approach to deduce T_e from the Langmuir probe I-V curve. The accuracy of this method depends on the accuracy of deducing the plasma potential (V_p).

b-iv) Electron density (n_e):

From the discussion of subsection a) it can be seen that n_e could be inferred from all the regions of the measured I-V characteristics curve. Different methods of deducing n_e from different regions of the measured I-V characteristics curve are summarized as follows:

1- Deducing n_e from ion saturation current region:

In this region ion density (n_i) could be deduced from equation 1 provided that T_e is known. Since the plasma is quasi-neutral medium then $n_e \approx n_i$

2- Deducing n_e from electron repelling current region:

Two methods could be used in this region for deducing n_e. First method is applied for Maxwellian electron energy distribution function. In this method, if the natural logarithms of the electron current ($Ln\ I_e$) is drawn against the applied voltage of the probe tip (V_a) a straight line is obtained. Then n_e is deduced using equation 3 provided that the plasma potential (V_p) is known. The accuracy of deducing n_e by this method is strongly dependant on the accuracy of deducing the plasma potential (V_p) and on the value of plasma potential because V_p in equation 3 is in the exponent of the exponential term of the equation. A little inaccuracy in the estimation of plasma potential at small value of V_p can lead to a big error in the value of the electron density. While a little inaccuracy in the estimation of plasma potential at big value of V_p can lead to a small error in the value of the electron density. To our knowledge, deducing n_e from equation 3 is a novel approach and has never been used before.

Second method is applied for Maxwellian and non-Maxwellian electron energy distribution functions. In this method, n_e could be deduced using equation 10 provided that $f(\varepsilon)$ is known. Henceforth, the electron density inferred using this method will be denoted as $n_{e(EEDF)}$.

3- Deducing n_e from the knee:

At the knee of the I-V curve, The plasma electron density can directly be obtained with the help of $I_{e,s}$ (random thermal current) once the value of plasma potential and the electron temperature is estimated. Since U = 0 at $V_a = V_p$. $I_{e,s} = (1/4)eA_p n_e v_{th}$ where $v_{th} = (8kT_e/\pi m_e)^{1/2}$. The random thermal current can be written as

$I_{e,s} = (1/2)eA_p n_e (2kT_e/\pi m_e)^{1/2}$ from which n_e can be deduced using the following relation

$$n_e = 5.91\times10^{18} T_e^{1/2} I_{e,s} \qquad (12)$$

where the units of T_e , $I_{e,s}$ and n_e are eV , A and m^{-3} respectively . From now on n_e deduced from the knee will be denoted by n_{eknee}.

The accuracy of this method is strongly dependent on the accuracy of the plasma potential estimation. A little inaccuracy in the estimation of plasma potential can lead to a big error in the value of the electron density due to the exponential behavior of the electron repelling current.

4- Inferring n_e from the electron current saturation region (OML region):

In the electron current saturation region, the square of the electron current is linear function of the probe biasing voltage and the slope of this relation is proportional to the square of the electron density. Therefore, n_e can be deduced using equation 6. Hereafter, the electron density inferred from this region will be denoted as n_{eOML}.

Experimental Setup:

The experimental setup is depicted in fig.2. The discharge chamber was a stainless steel cylinder with inner diameter of 310 mm and it was evacuated by using 250 l/s (liter / second) turbo molecular pump backed up by

mechanical rotary pump, and its base pressure was maintained below $5x10^{-6}$ Torr. The gas inlet was at the center of the chamber and the flow was controlled using a mass flow controller. Pure argon gas was used at fixed pressure of 20 mTorr with flow rate of 132 sccm.

The plasma was generated and sustained by planar, spiral, three turns water-cooled copper coil antenna. The coil was located behind a 25 mm thick quartz window. The discharge was maintained between the quartz window and a grounded stainless steel end plate, which were separated by 75 mm, all the measurements were performed midway between the quartz window and the stainless steel end plate. A pulse-modulated RF current of frequency 13.56 MHz was used to derive the inductive electric field which produced the discharge. The RF modulation frequency was 12.5 kHz and the duty cycle was 50%. The average input power measured before the matching network was fixed at 300 & 500 W (600 & 1000 W in the glow phase) and the reflected power was kept around 5 W.

The probe measurements were performed using a single cylindrical Langmuir probe (having a Pt tip) with radius of 500 μm and length of 1 mm. The probe was inserted into the discharge chamber from the sidewall of the chamber at the center between the grounded end plate and the quartz window. In order to protect the I-V probe characteristics from RF distortion, two RF resonance filters with resonance frequencies of 13.56 and 27.12 MHz, respectively, were closely connected to the probe tip, minimizing the stray capacitance. The probe in this case is called passively compensated Langmuir probe. The theory of probe compensation is beyond the scope of this article.

The boxcar sampling technique was used for the time resolved measurements in the pulsed ICP. The probe voltage was swept in a range from –50 V to +30 V, and the probe current was measured through a differential amplifier from the voltage drop across a 10 Ω resistor. The probe voltage and current were obtained with an AD-converter card which provided 16-bit resolution and a sampling frequency of 500 k samples/s. The trigger signal from an arbitrary waveform generator synchronized the probe data acquisition system with the pulsed RF power supply. The reference point of the trigger was chosen as the time when the RF power was turned off, defining the initial time ($\tau = 0$). The time resolution of the probe acquisition system was 1 μs. In order to improve the signal-to-noise ratio, a 100 sweeps of the probe voltage were performed, which were averaged.

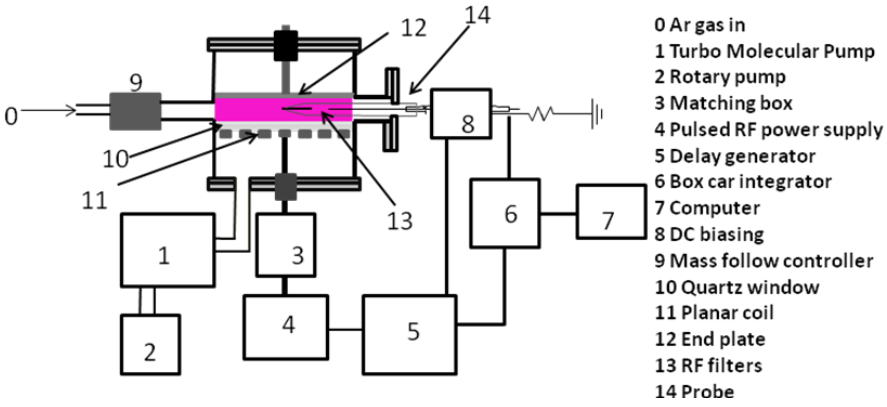

Fig. 2: Experimental setup.

RESULTS AND DISCUSSION

The measured I-V curves of the electric probe in the afterglow of discharge power of 500 & 300 watts are depicted in figures 3 (a) & 3 (b) respectively. From these figures it is clearly seen that the I-V curves are almost ideal since the electron saturation region is obtained. Also, it is clearly seen that the probe currents at the knees in figure 3 (a) are almost 20 folds that shown in figure 3 (b) which indicates that n_e of conditions shown in figure 3 (a) is almost an order of magnitude higher than that shown in figure 3 (b).

The temporal behaviors of V_p & V_f in the afterglow for the conditions of figures 3 (a) & 3 (b) is shown in figure 4. This temporal behavior is reasonable for decaying plasmas in the afterglow. For the first 15 μs in the afterglow, V_p is linearly decreased while it is monotonically decreased in the rest of the afterglow time. The afterglow values of V_p are almost the same for discharge powers of 500 & 300 Watts. Similar data were obtained in (Singh, 2004) in 10 mTorr argon ICP discharge where V_p values were almost constant in RF power range of 77 - 245 Watts. The temporal behavior of V_f of 500 watt discharge follows the behavior of V_p and this is understood because for collisionless sheath around the electric probe the following relation is valid (Chen,

Australian Journal of Basic and Applied Sciences, 10(18) December 2016, Pages: 290-302

2003) $\frac{V_p - V_f}{T_e} = 4.7$ where T_e is in volts, in the case of argon plasmas. This relation suggests that V_f should decrease when V_p is decreased and T_e is constant. Also, it suggests that V_p-V_f should decrease whenever T_e is decreasing. Therefore, for small decrease in V_p and bigger decrease in T_e then V_f should decrease. Different trend of V_f in the afterglow was obtained in the case of 300 watt discharge where V_f shows an increase at τ of 5 & 7 μs. This can be explained as follows: Both of T_e & V_p values at τ of 5 & 7 μs were smaller than their values at 3 μs. T_e (5 & 7 μs)/T_e (3 μs) is less than V_p (5 & 7 μs)/V_p (3 μs), accordingly V_f (5 & μs) should increase compared with V_f (3μs) to maintain the validity of the relation $\frac{V_p - V_f}{T_e} = 4.7$

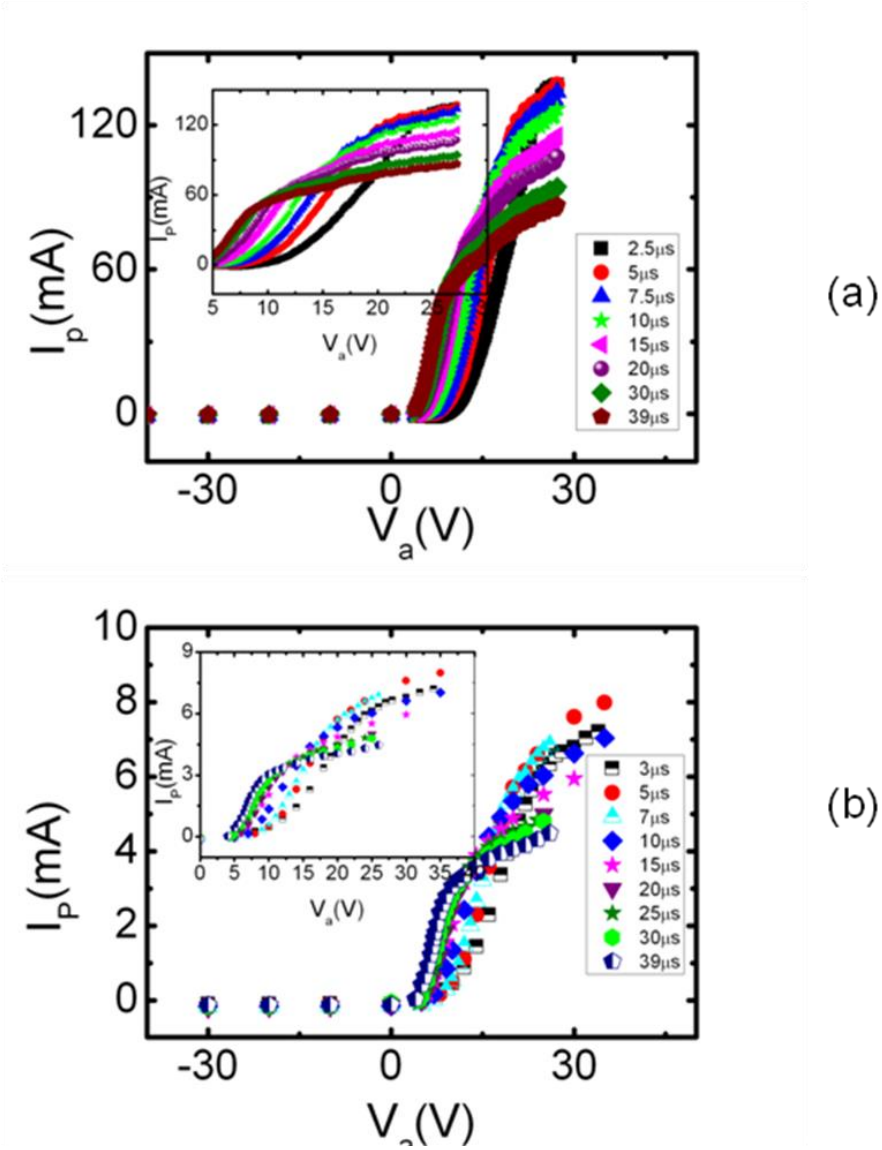

Fig. 3: Temporal evolutions of Langmuir probe's I-V curves in the afterglow (a) 500 Watt & (b) 300 Watt.

Australian Journal of Basic and Applied Sciences, 10(18) December 2016, Pages: 290-302

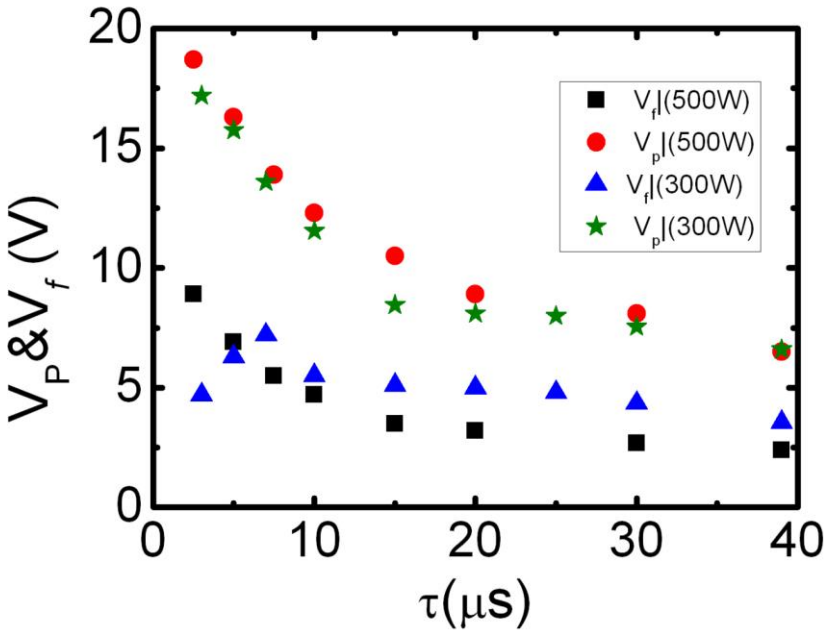

Fig. 4: Temporal evolutions of plasma potential Vp & floating potential Vf for average discharge powers of 300 & 500 Watts.

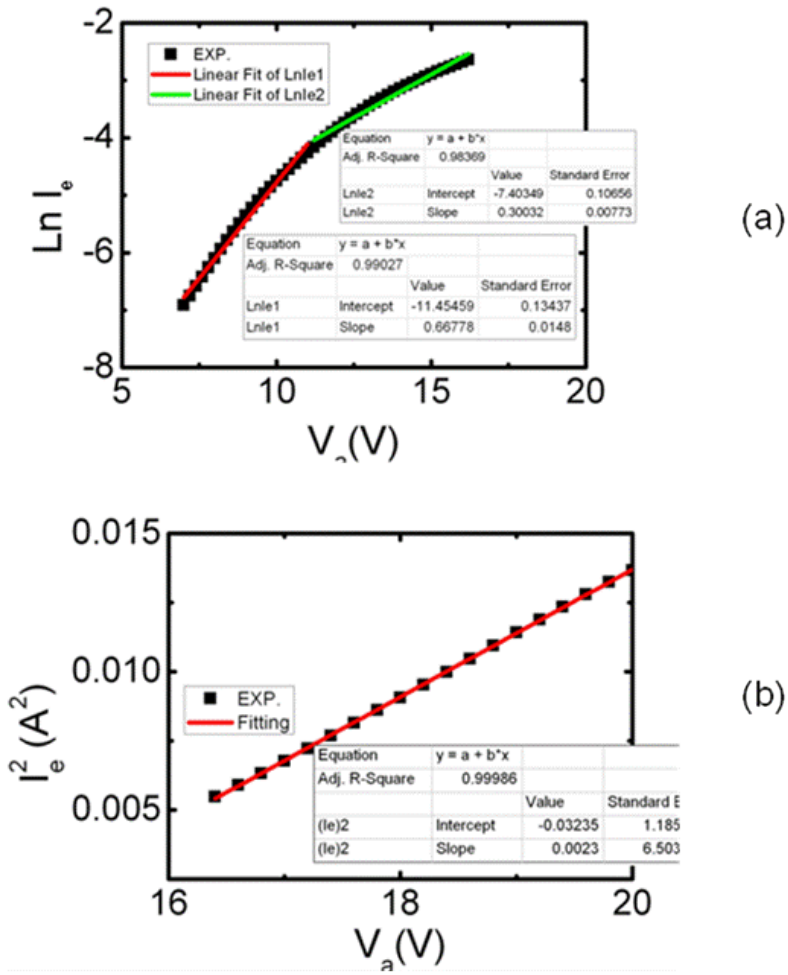

Fig. 5: Relation between (a) LnI_e versus V_a and (b) $(I_e)^2$ versus V_a . Averaged RF power was 500 watt and the probe I-V curve was measured at 5 μs in the afterglow.

The main goal of the current article is to use novel approaches to estimate T_e & n_e from the electron saturation current & the electron repelling current regions of the probe's I-V curve respectively, and comparing their values with the values that estimated using standard well known approaches. Figures 5 (a) & 5 (b) show the relation between V_a & Ln I_e (in the electron repelling region) and between V_a & I_e^2 (in the OML region) respectively, where the RF power was 500 watt at τ of 5 μs. Figure 5(a) shows that the relation between V_a & Ln I_e is not straight line but it can be fitted by two straight lines which mean that the electron energy distribution function is bi-Maxwellian (the plasma has two group of electron). The slope and the intersection of each fitted line in figure 5 (a) is used in equation 3 to calculate the electron density of each group of electrons. The group which have lower T_e is called cold temperature group (its electron density is n_{ec} & its electron temperature is T_{ec}) and the group which have higher T_e is called hot temperature group (its electron density is n_{eh} & its electron temperature is T_{eh}). Figure 5 (b) shows that the relation between V_a & I_e^2 is straight line, therefore the slope and the intersection of the fitted line is used in equation 8 to calculate T_e. It should be mentioned here that in the entire period of the afterglow, the electron energy distribution function of 500 watt plasma was bi-Maxwellian while it was Maxwellian in the case of 300 watt plasma.

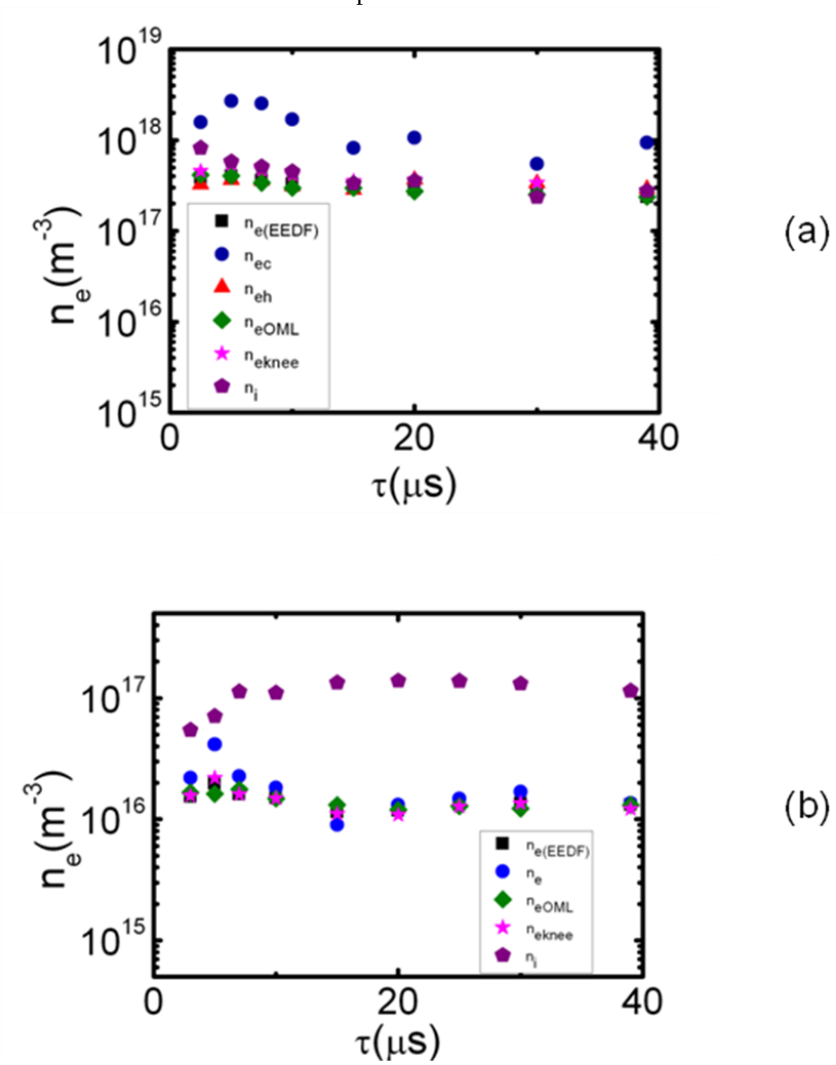

Fig. 6: Temporal evolutions of n_e inferred from the different regions of Langmuir probe's I-V curves. (a) RF averaged power of 500 watt & (b) RF averaged power of 300 watt.

The temporal evolutions of the electron densities (inferred from the different regions of the measured I-V curves) of 500 watts and 300 watts plasmas are depicted in figures 6 (a) & 6 (b) respectively. Figures 6 (a) & 6 (b) show that the electron densities which inferred from the different regions of the measured I-V curves of 500 watts plasma are an order of magnitude higher than that of 300 watts plasma.

The trends of the electron densities of 500 watts & 300 watts plasmas show an increase in the values of n_{ec}, n_{eh}, n_{eknee}, $n_{e(EEDF)}$ and n_{eOML} at τ = 5 μs except n_i that inferred from the ion saturation region. The increase of the value of n_e in the afterglow might be ascribed to Penning ionization (equation 13) or inelastic collision of

electron (having energy > 4.2 eV) with metastable argon atom (Ar*) (equation 14) (ElSabbagh *et al*., to be published, Blessington, 2007).

$$Ar^* + Ar^* \rightarrow Ar^+ + Ar + e_P \quad (13)$$

$$Ar^* + e_f \rightarrow Ar^+ + e + e \quad (14)$$

Where e_P & e_f are electrons having energies of 7.3 eV & energy > 4.2 eV respectively and e is electron having low energy. The overall effect of equations 13 & 14 is to enhance the electron density in the afterglow. The reactions represented by equations 13 & 14 could be enhanced by super-elastic collisions (equation 15) (ElSabbagh, 2003). In super-elastic collision a fast electron e_S (energy > 11.5 eV) is produced from the elastic collision of low energy electron with Ar*.

$$Ar^* + e \rightarrow Ar + e_S \quad (15)$$

The overall effect of reactions that represented by equations 13, 14 & 15 is the modifications of the electron energy distribution function in the neighborhood of the energies 4.2 eV, 7.3 eV & 11.5 eV as can be seen from $f(\varepsilon)$ that is shown in figure 8. Ar* atoms in equations 13,14 & 15 are produced in the glow phase of the discharge.

Figure 6 (a) shows a good agreement among n_{eh} , n_{eknee} , $n_{e(EEDF)}$ and n_{eOML} while n_{ec} which inferred from the electron repelling current region is almost an order of magnitude higher at the first 10 μs of the afterglow period. The disagreement between n_{ec} and n_{eknee}, $n_{e(EEDF)}$ & n_{eOML} should suggest that the inferring of n_e from the electron repelling current region of the probe's I-V curve using equation 3 is not appropriate method. Laser Thomson scattering (LTS) measurements (ElSabbagh et al., to be published) of n_e for the same discharge conditions of the current article show that $f(\varepsilon)$ of 500 watt discharge conditions are bi-Maxwellian and the values & the temporal behavior of the cold group of electrons n_{ec} have a good agreement with that shown in figure 6(a) of the current article. LTS is an independent technique for measuring $f(\varepsilon)$, n_e and T_e (ElSabbagh, 2003) and does not need any model to infer n_e, T_e & $f(\varepsilon)$. Therefore the good agreement between n_{ec} measured by LTS and that inferred from the electron repelling current region of the probe's I-V curve gives high confidence of inferring n_e from the electron repelling current region. It should be mentioned here that the inferring of n_e from the electron repelling region of the probe's I-V curve is the only direct method to deduce n_{ec} & n_{eh} of plasmas having bi-Maxwellian $f(\varepsilon)$ rom Langmuir probe's I-V curve. Figure 6 (b) shows a good agreement among all the electron densities except n_i which inferred from the ion saturation region where n_i is almost an order of magnitude higher at the last 25μs of the afterglow.

The temporal evolutions of T_e (inferred from the different regions of the measured I-V curves) of 500 watts and 300 watts plasmas are shown in figures 7 (a) & 7 (b) respectively. It is clearly seen from these figures that the electron temperatures are decreasing with the elapsed time in the afterglow except T_{eOML} shown in figure 7 (a) where T_{eOML} is linearly increased with time in the first 10 μs and it decreases after that. The failure of T_{eOML} to follow the temporal behavior of T_{eeff}, T_{eh} & T_{ec} could be attributed to the fact that I_e^2 against V_a in the electron current saturation region is single straight line which gives single value for both of the slope & C_2 of equation 7. Therefore, T_{eOML} deduced from equation 7 for plasma having bi-Maxwellian $f(\varepsilon)$ will have single value which lies between T_{eh} & T_{ec}. More theoretical studies should be conducting to know the effect of cold and hot group of electrons on the electron current of the electron saturation region.

From figure 7 (a) it can be noticed that there is a good agreement between T_{eeff} & T_{eh} in the first 10 μs of the afterglow while there is a good agreement between T_{ec} & T_{eOML} and fair agreement between T_{eeff}& T_{eh} in the last 20 μs in the afterglow. The electron temperatures (T_{eeff}, T_{eOML} & T_e) shown in figure 7 (b) have similar trends where they are decreasing as τ increasing, also there is a fair agreement among their values especially at the last 25 μs of the afterglow. The fair agreement between T_{eOML} and T_{eeff} & T_e is due to the fact that $f(\varepsilon)$ of the conditions of figure 7 (b) is Maxwellian.

Conclusion:

The temporal evolutions of n_e & T_e in the afterglow of pulse-modulated argon ICP were measured using compensated Langmuir probe. The measurements were performed for averaged RF powers of 300 & 500 Watts. The electron temperature was found to decrease rapidly in the first 10 μs and after that it was found that it was decreasing monotonically in the rest of the afterglow period. The electron density was found to have a peak value at τ = 5 μs and after that it was found to be decreasing monotonically. The peak value of the electron density could be attributed to Penning ionization.

For the first time, two novel approaches have been proposed and checked to infer n_e & T_e from the electron repelling current and electron saturation current regions of the measured compensated-Langmuir probe's I-V curve respectively. Inferring n_e from the electron repelling current region has been proved to be a reliable approach, and it is the only approach to deduce the electron densities of cold & hot groups of plasmas having bi-Maxwellian electron energy distribution function. Inferring T_e from the electron saturation current region has

been found to be reliable method only in case of plasmas having Maxwellian electron energy distribution function.

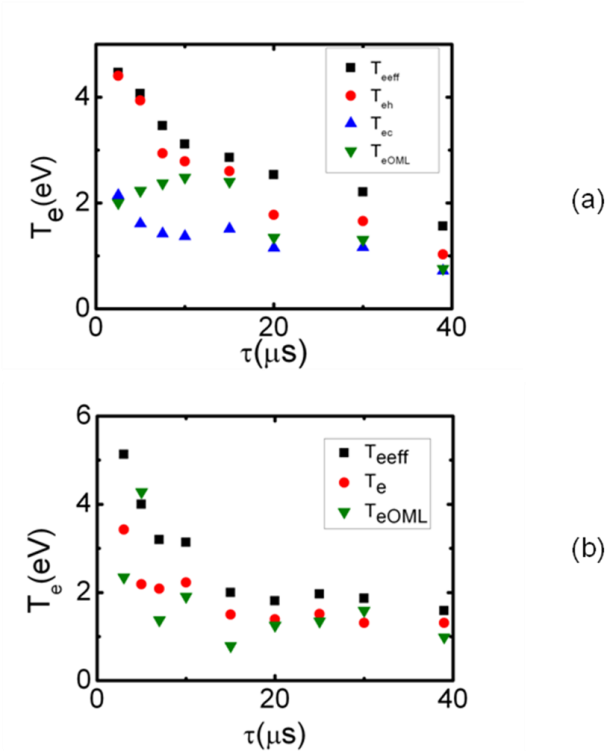

Fig. 7: Temporal evolutions of T_e inferred from the different regions of Langmuir probe's I-V curves. (a) RF averaged power of 500 watt & (b) RF averaged power of 300 watt.

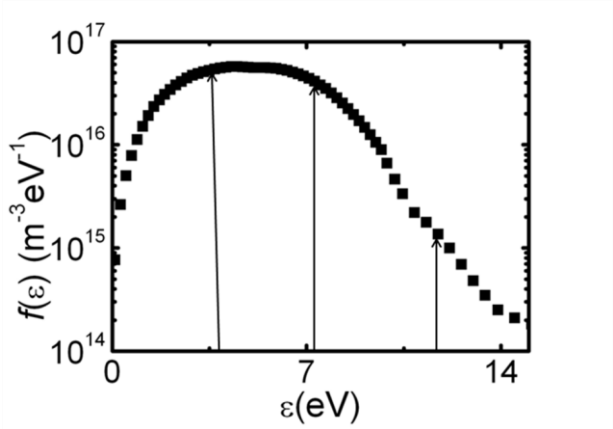

Fig. 8: Modification of electron energy distribution function at energies 4.2 eV, 7.3eV & 11.5 eV due to reactions represented by equations 13, 14 & 15. RF averaged power of 500 watt and t of 7.5 μs.

REFERENCES

Blessington, J.C., 2007. Measurements of metastable atom density using energies and densities of energetic "fast" electrons detected in the electron energies distribution function associated with afterglow plasma produced by radio frequency inductively coupled helium discharge, Master thesis, West Virginia University, USA.

Chen, F.F., 1965. Plasma Diagnostic Techniques. Editted by Huddlestone R. H., and Leonard S. L. New York: Academic Press.

Chen, F.F., 1983. Introduction to Plasma Physics and Controlled Fusion. Plenum Press.

Chen, F.F., 2003. Lecture Notes on Langmuir Probe Diagnostic., Mini-Course on Plasma Diagnostics, IEEE-ICOPS meeting, Jeju, Korea.

Despiau-Pujo, E., M. Brihoum, G. Cunge, M. Darnon, N. Braithwaite and O. Joubert, 2013. Pulsed ICP plasmas processing : A combined modelling and experimental study. In the proceeding of 31st ICPIG, Granada, Spain.

Economou, D.J., 2016. Pulsed plasma etching for semiconductor manufacturing. Journal of Physics D: Applied Physics, 47(30): 303001.

ElSabbagh, M.A.M., 2003. Study of Electron Properties of a Capacitively Coupled RF Argon Plasma by Laser Thomson Scattering, Ph.D. dissertation, Kyushu University, Japan.

ElSabbagh, M.A.M., Yamagata Y. and Uchino K., to be published.

Gagne, R.R.J. and A. Cantin, 1972. Investigation of an rf Plasma with Symmetrical and Asymmetrical Electrostatic Probes, Journal of Applied Physics, 43(6): 2639.

Hershkowitz, N., M.H. Cho, C.H. Nam and T. Intrator, 1988. Langmuir probe characteristics in RF glow discharges Plasma Chem. Plasma Processes, 8(1): 35.

Hershkowitz, N., 1989. Plasma Diagnostics. Editted by Auciello O. and Flamm D. New York: Academic press.

Hershkowitz, N., 2016. 43 Years of Fun Basic Plasma Physics Experiments, IEEE Transaction on Plasma Science, 44(4): 347.

Langmuir, I., Mott-Smith, Harold Jr., 1924. Studies of electric discharges in gases at low pressures, General Electric Review, 27: 449.

Laurent, C.P., J. UloUP, B.P. Caillier, L. Thérèse and Ph. Guillot, 2013. Spatial characterization of an inductively coupled plasma in argon with optical emission spectroscopy and Langmuir probe diagnostics for surface treatment purpose, In the proceeding of 31st ICPIG, Granada, Spain.

Lee, J., K. Kim, D. Kim and C. Chung, 2016. The radio-frequency fluctuation effect on the floating harmonic method Physics of Plasmas, 23(8): 083517.

Liu, L., S. Sridhar, V.M. Donnelly, D.J. Economou, 2015. Ignition delay of a pulsed inductively coupled plasma (ICP) in tandem with an auxiliary ICP. Journal of Physics D: Applied Physics, 48(48): 485201.

Lobbia, R.B. and A.D. Gallimore, 2010. Temporal limits of a rapidly swept Langmuir probe, Physics of Plasmas, 17(7): 073502.

Malyshev, M.V. and V.M. Donnelly, 2000. Dynamics of inductively-coupled pulsed chlorine plasmas in the presence of continuous substrate bias, Plasma Sources Science and Technology, 9(3): 353.

Meshcheryakova, E., M. Zibrov, A. Kaziev, G. Khodachenko and A. Pisarev, 2015. Langmuir Probe Diagnostics of Low pressure Inductively Coupled Argon Plasmas in a Magnetic Field. Physics Procedia, 71: 121.

Messerer, P., 2010. Investigation and development of plasma surfaces processes: Etching of semiconductors and sterilization of polymers, Ph.D. dissertation, Ruhr University, Bochum, Germany.

Paranjpe, A.P., J.P. McVittie and S.A. Self, 1990. A tuned Langmuir probe for measurements in rf glow discharges Journal of Applied Physics, 67(11): 6718.

Petit-Etienne, C., M. Darnon, L. Vallier, E. Pargon, G. Cunge, F. Boulard, S. Banna, T. Lill and O. Joubret, 2010. Reducing damage to Si substrates during gate etching processes by synchronous plasma pulsing, Journal of Vacuum Science and Technology, 28(5): 926.

Ramamurthi, B., D.J. Economou and I.D. Kaganovich, 2003. Effect of non-local electron conductivity on power absorption and plasma density profiles in low pressure inductively coupled discharges, Plasma Sources Science and Technology, 12(2): 170.

Singh, S.V., 2004. Investigation of ICP RF discharges by means of a Langmuir probe, Ph. D. dissertation, Ruhr University, Bochum, Germany.

Sudit, I.D. and F.F. Chen, 1994. RF compensated probes for high-density discharges. Plasma Sources Science and Technology, 3(2): 162.

Sugai, H., K. Nakamura, Y. Hikosaka and M. Nakamura, 1995. Diagnostics and control of radicals in an inductively coupled etching reactor. Journal of Vacuum Science and Technology A, 13(3): 887.

Swift, J.D. and M.J.R. Schwar, 1971. Electrical Probes for Plasma Diagnostics. New York: Elsevier.

Watanabe, Y., M. Shiratani, Y. Kubo, I. Ogawa and S. Ogi, 1988. Effects of low-frequency modulation on rf discharge chemical vapor deposition, Applied Physics Letter, 53(14): 1263.